

## Contribution of Wing, Vertical Tail and Fuselage on Airplane Stability with Failed Outboard Engine

Dr.Mohamed.A.R.Yass \*, Naseer H. Farhood  Raed Abbas Jessam\*

Received on: 8/9/2008

Accepted on: 5/3/2009

### Abstract

The Effect of wing, vertical tail, and fuselage design parameters on airplane stability with failed outboard engine presents in this study. Boeing (747-400) have been selected for available data. The semi empirical equations (Datacom) have been used with modification of unbalance engines thrust. It had been seen that the wing sweep angle had negative effect but the vertical tail sweep angle had a positive effect toward directional and lateral stability and other results established by using modified datacom computer program which could be used as a real design requirements for further configuration improvements of the airplane.

**Keywords:** Wing; Vertical tail; Fuselage; Airplane stability

### مساهمة الجناح، الذيل العمودي والجسم على استقرارية الطائرة عند فشل إحدى المحركات الخارجية

#### الخلاصة

تم في هذا البحث دراسة بعض العوامل التصميمية للجناح والجسم والذيل العمودي على الاستقرارية الاتجاهية والدورانية في حالة عطل احد المحركات الخارجية للطائرات المدنية حيث تم اختيار طائرة البوينغ (747-400) لتوفر المعلومات باستخدام المعادلات التجريبية (Datacom) أن إضافة تأثير عدم توازن المحركات وقد تبين أن زاوية تراجع الجناح تؤثر بشكل سلبي بينما زاوية تراجع الذيل العمودي تؤثر بشكل ايجابي على الاستقرارية الاتجاهية والدورانية وي طرح البحث مجموعه من النتائج التي تم الحصول عليها بعد تطوير برنامج Datacom التي يمكن أخذها بنظر الاعتبار من العوامل التصميمية في تصاميم الطائرات المدنية.

### Nomenclature

$b$	Wing span	ft
$\Delta C_{Lcc}$	Change in vertical tail $C_L$ due to circulation control	-----
$D_{ewm}$	Drag due to wind milling of failed engine	Ib
$K_f$	Fuselage correction factor	-----
$K_{MA}$	Compressibility correction to sweep	-----
$K_{MT}$	Compressibility correction to dihedral	-----
$K_N$	Empirical factor for body and body with wing effects	-----

$K_{Rl}$	Reynold's number factor for the fuselage	-----
$K_{wb}$	Factor for fuselage loss in the lift curve slop	-----
$l_{tv}$	Horizontal distance between CG and engine nozzle	ft
$l_{vtail}$	Horizontal distance between CG and aerodynamic center of vertical tail	ft
$M$	Mach Number	-----
$q$	Dynamic pressure at the engine-out flight condition	$\frac{Kg}{m.s^2}$
$S_o$	Cross-sectional area of fuselage	$ft^2$
$S_{ref}$	Wing reference area	$ft^2$
$S_{vtail}$	Vertical tail area	$ft^2$
$T_o$	Static thrust at sea level	$lb_f$
$Y_{ext}$	External side force	$lb$
$z_{tv}$	Vertical distance between CG and engine nozzle	ft
$z_{vtail}$	Vertical distance between CG and aerodynamic center of vertical tail	ft
$\alpha$	Angle of attack	rad.
$\beta$	Sideslip angle (positive with relative wind from right)	rad
$b_M$	Compressibility factor = $\sqrt{1 - M^2}$	rad
$d_a$	Aileron deflection (positive for right up, left down)	rad
$d_r$	Rudder deflection (positive right)	rad
$e$	Downwash angle	rad
$f$	Bank angle (positive right roll )	rad
$h_{htail}$	Dynamic pressure ratio at the horizontal tail	-----
$k$	Ratio of actual lift curve slope to $2p$	-----
$s$	Ratio of density at a given altitude to density at sea level	-----
$\Lambda_{c/4}$	Quarter-chord sweep angle	rad
$\Lambda_{c/2}$	Half-chord sweep angle	rad
$\Gamma$	Dihedral angle	rad

**1.Introduction**

One of the major problem in the aircraft is maintains steady flight if one failed outboard engine,[1] .this paper discuss the contribution of wing vertical tail and fuselage by using datacom method,[2]. And the establishment of the engine out constraint based on the required yawing moment coefficient. The use of thrust vectoring and circulation control to provide additional yawing moment is also described,[3].

The coefficients of the variables and their derivatives are seen to be dependent upon a large number of factors. These factors are describing the geometry of vehicle and other factor describes the speed of vehicle at which the failure occurs,[4]. The last group of terms is composed of the rates of change of the rolling moment coefficient and vibration of sideforce coefficient and vibration of yawing moment coefficient. These terms were introduced into the original equations of stability Fig. (1),[4].

**2. Mathematical Analysis**

The estimation of stability and control derivatives for outboard engine constraint depend thrust vectoring and circulation control which can be determined from the sideforce, rolling and yaw moment contribution using the Roskam method,[1]. The stability and control derivatives which illustrated the above analysis are formulated in the following equations.

Boeing (747-400) had been selected for available data Figure (2).

**2.1 Sideforce equation**

In a conventional control system, the vertical tail is the dominant controller for generating a yawing moment, [1].

$$C_{y_{da}}d_a + C_{y_{dr}}d_r + C_{y_b}b + C_L \sin f \tag{1}$$

$$-\frac{T \sin e}{qS_{ref}} - \Delta C_{Lcc} \frac{S_{vtail}}{S_{ref}} = -\frac{Y_{ext}}{qS_{ref}}$$

Wher

e:  $C_{y_{da}}, C_{y_{dr}}, C_{y_b}$  Variation of sideforce coefficient with aileron deflection, rudder deflection and yaw angle respectively.

However, thrust vectoring and circulation control can be used to generate additional yawing moments. Since the engine out condition is critical constraint for a truss braced wing with tip mounted engines, the capability to model thrust vectoring and circulation control on the vertical tail also determine. The fifth term in the equation above ( $\frac{T \sin e}{qS_{ref}}$ ) is due to the

thrust being vectored at an angle ( $e$ ) to the centerline, and the sixth term ( $\Delta C_{Lcc} \frac{S_{vtail}}{S_{ref}}$ ) is due to the change in

( $C_L$ ) at the vertical tail due to circulation control. Since the external sideforce ( $Y_{ext}$ ) is zero, and ( $C_{y_{de}}$ ) is assumed to be zero, this equation can be simplified and solved for the sideslip angle,[1].

$$b = \frac{-C_{y_{dr}}d_r - C_L \sin f + \frac{T \sin e}{qS_{ref}} + \Delta C_{Lcc} \frac{S_{vtail}}{S_{ref}}}{C_{y_b}} \tag{2}$$

The aileron deflection required to maintain equilibrium flight is obtained by summing the rolling moments about the x-axis.

**2.2 Rolling moment equation**

By setting the external rolling moment ( $L_{ext}$ ) equal to zero, this equation can be solved for the aileron deflection,[2].

$$Cl_{da}d_a + Cl_{dr}d_r + Cl_b b - \frac{T \sin e}{qS_{ref}} \frac{z_{tv}}{b} - \Delta C_{Lcc} \frac{S_{vtail}}{S_{ref}} \frac{z_{vtail}}{b} = -\frac{L_{ext}}{qS_{ref}b} \tag{3}$$

$$d_a = \frac{-Cl_{dr}d_r - Cl_b b + \frac{T \sin e}{qS_{ref}} \frac{z_{tv}}{b} + \Delta C_{Lcc} \frac{S_{vtail}}{S_{ref}} \frac{z_{vtail}}{b}}{Cl_{da}} \tag{4}$$

Where:  $Cl_{da}$ ,  $Cl_{dr}$ ,  $Cl_b$  are the variation of rolling moment coefficient with aileron deflection, rudder deflection and yaw angle respectively.

The rudder deflection is initially set to the given maximum allowable steady state value, and the sideslip angle and aileron deflection for equilibrium flight are determined by equations (2) and (4). The maximum allowable steady state deflection is typically ( $20^\circ - 25^\circ$ ). This allows for an additional ( $5^\circ$ ) of deflection for maneuvering, [7].

The maximum available yawing moment is found by summing the contribution duo to the ailerons, rudder and sideslip.

**2.3 Yawing moment equation**

The value of the available yawing moment coefficient is then constrained

in the optimization problem to be greater than the required yawing moment coefficient, [6].

$$Cn_{avail} = Cn_{da}d_a + Cn_{dr}d_r + Cn_b b + \frac{T \sin e}{qS_{ref}} \frac{l_{tv}}{b} + \Delta C_{Lcc} \frac{S_{vtail}}{S_{ref}} \frac{l_{vtail}}{b} \tag{5}$$

Where:  $Cn_{da}$ ,  $Cn_{dr}$ ,  $Cn_b$  are the variation of yawing moment coefficient with aileron deflection, rudder deflection and yaw angle respectively.

This is far below the angle of attack corresponding to the maximum lift coefficient of a typical vertical tail. It could be expect that the maximum available yawing moment is obtained when the vertical tail is flying at its maximum lift coefficient, but this is not true, because the equilibrium equations above must always be satisfied for steady flight. To illustrate this point, equation (1) has been solved for the bank angle with no thrust vectoring and no circulation control,[8].

$$f = \sin^{-1} \left[ -\frac{(Cy_{dr}d_r + Cy_b b)}{C_L} \right] \tag{6}$$

**2.4 Sideforce coefficient**

The variation of sideforce coefficient with sideslip angle has contributions from the wing, fuselage, and vertical tail, [8].

$$Cy_b = Cy_{bwing} + Cy_{bfuse} + Cy_{bvtail} \tag{7}$$

The wing contribution is a function of the dihedral

$$Cy_{bwing} = -0.0001 |\Gamma| \frac{180}{p} \tag{8}$$

The fuselage and nacelle contributions are estimated by:

$$C_{y_{bfuse}} = -2 K_{wbi} \frac{S_o}{S_{ref}} \quad (9)$$

Where: ( $K_{wbi}$ ) is the wing body interference factor, [1]

### 2.5 Rolling moment coefficient due to SideSlip

The variation of rolling moment coefficient with sideslip angle has contributions from the wing body, horizontal tail, and vertical tail,[8].

$$C_l_b = C_{l_{bwb}} + C_{y_{bh tail}} + C_{y_{bv tail}} \quad (10)$$

The contribution from the wing body is estimated by,[3]

$$C_{l_{bwb}} = \left[ C_L \left( \left( \frac{C_{l_b}}{C_L} \right)_{\lambda/2} K_{MA} K_f + \left( \frac{C_{l_b}}{C_L} \right)_A \right) \right] \frac{180}{p} + \left[ \Gamma \left( \frac{C_{l_b}}{\Gamma} K_{Mf} + \frac{\Delta C_{l_b}}{\Gamma} \right) + (\Delta C_{l_b}) z_w \right] \quad (11)$$

The contribution from the horizontal tail is approximately zero, since it has a small lift coefficient, small dihedral, and small area relative to the wing.

$$C_{l_{bh tail}} = 0 \quad (12)$$

The contribution from the vertical tail is estimated by,[8]:

$$C_{l_{bv tail}} = C_{y_{bv tail}} \frac{(z_{v tail} \cos \alpha - l_{v tail} \sin \alpha)}{b} \quad (13)$$

### 2.6 Yawing moment coefficient due to SideSlip

The variation of yawing moment coefficient with sideslip angle has

contributions from the wing, fuselage, and vertical tail,[8].

$$C_{n_\beta} = C_{n_{bwing}} + C_{n_{bfuse}} + C_{n_{bv tail}} \quad (14)$$

The wing contribution to the yawing moment coefficient is negligible for small angles of attack.

$$C_{n_{bwing}} \cong 0 \quad (15)$$

The fuselage contribution to the yawing moment coefficient is determined by,[2]:

$$C_{n_{bfuse}} = -K_N K_{RI} \frac{S_{bs}}{S_{ref}} \frac{l_{fuse}}{b} \frac{180}{p} \quad (16)$$

The contribution from the vertical tail is estimated by the following equation,[2].

$$C_{n_{bv tail}} = -C_{y_{bv tail}} \frac{(l_{v tail} \cos \alpha + z_{v tail} \sin \alpha)}{b} \quad (17)$$

### 2.7 Rolling moment coefficient due to Rudder Deflection

The variation of rolling moment coefficient with rudder deflection is given by,[1]:

$$C_{l_{dr}} = C_{y_{dr}} \left( \frac{z_{v tail} \cos \alpha - l_{v tail} \sin \alpha}{b} \right) \quad (18)$$

### 2.8

### Yawing moment coefficient due to Rudder Deflection

The variation of yawing moment coefficient with rudder deflection is given by,[2]:

$$C_{n_{dr}} = -C_{y_{dr}} \frac{(l_{v tail} \cos \alpha + z_{v tail} \sin \alpha)}{b} \quad (19)$$

## 3.Results & Discussion

Wing surface Area ( $S_{ref}$ ) it had positive effect toward yaw and lateral stability due to negative slope with  $C_{n_\beta}$  and positive slope with  $C_{l_\beta}$  because wing

surface Area(  $S_{ref}$  ) always increases lift(Fig(3),Fig(4)).

Increases of wing sweep angle lateral and directional stability decreases as shown ( Fig (5) , Fig (6) ) due to positive slope with  $C_{n\beta}$  and negative slope with  $Cl_{\beta}$  because wing sweep angle shifted aerodynamic center back and decrease the lift.

Upper wing location decreases the lateral and directional stability for the same reason mention above, (Fig (7), Fig (8)).

Wing dihedral had no effect on directional stability due to zero slopes with  $C_{n\beta}$  because it doesn't generate any extra sideforce. And also it had no effect on the aerodynamic center and it had little effect on lift and negative effect on lateral stability due to negative slope with  $Cl_{\beta}$ , because it generate extra couple around the x-axis(Fig(9), Fig(10)).

Fuselage diameter had positive effect to directional stability and negative effect toward lateral stability because it increase the couples arm toward lateral stability (x-axis) and increase diameter request more force to rotate fuselage around y-axis (directional stability), [ Fig (11), Fig (12)].

As shown in Fig (13) vertical tail tip chord had positive slope with  $C_{n\beta}$  and that mean negative effect toward directional stability and from Fig (14) it had same behavior toward lateral stability.

Vertical tail tip and vertical tail root had exactly same behavior toward directional and lateral stability (Fig (15) ,(Fig (16))). The increases of vertical tail sweep angle had positive

toward lateral and directional stability as shown in Fig (17) , Fig (18). this was all because increase lift of vertical tail which would be more powerful toward lateral and directional stability(Fig(1)). Airplane speed had positive effect to directional stability and negative effect to lateral stability, (Fig (19), Fig (20)) because had two component one toward x-axis (lateral stability) and other against y-axis (directional stability).

#### 4. Conclusion

Airplane outboard engine failure is danger without proper care design and it becomes very serious with two engine airplane one on each side.

Wing area, sweep angle, wing location, dihedral and fuselage design are part of solution but the major solution of airplane outboard engine failure was the vertical tail with powerful rudder device and limited airplane speed.

#### Reference

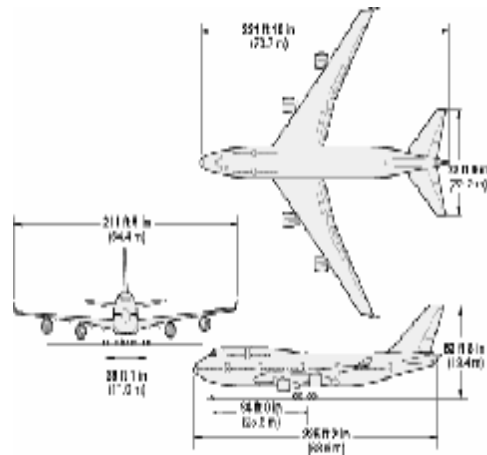
- [1] Roskam, J., *Methods for Estimating Stability and Control Derivatives Conventional Subsonic Airplanes*, Roskam Aviation and Engineering Corporation, Lawrence, Kansas, 1971.
- [2] Hoak, D.E. et al., *USAF Stability and Control DATCOM*, Flight Control Division, Air Force Flight Dynamics Laboratory, WPAFB, Ohio, 1978.
- [3] Torenbeek, E., "Synthesis of Subsonic Airplane Design ", Kluwer Academic, 1998.
- [4] Hanke, C.R., "The Simulation of a Large Jet Transport Aircraft, Vol. I:Mathematical Model," NASA CR-1756, March 1971.

[5] Etkin, B., "Dynamics of Flight, Stability and Control ", John Wiley & Sons, Inc 2003.

[6] Nelson, R. C., *Flight Stability and Automatic Control*, McGraw-Hill Co., New York, 1989.

[7] MacMillin, P.E., Golovidov, O.B., Mason, W.H., Grossman, B., and Haftka, R.T., *Trim, Control, and Performance Effects in Variable-Complexity High-Speed Civil Transport Design*, MAD 96-07-01, July, 1996.

[8] Heffley, R.K., and Jewell, W.F., *Aircraft Handling Qualities Data*, NASA CR- 2144, December, 1972.



7.0 deg.	dihedral wing
6.2 ft	z_wing
23.0 ft	dia_fuse
5500 ft <sup>2</sup>	S(ref)
33.5 ft	hspan_vtail
14.4 ft	depth_fuse_vtail
36.4 ft	c_vtail_root
11.5 ft	c_vtail_tip
0.25	Mach_
45 deg.	sweep_vtail_1_4
33.5 deg.	sweep_wing_1_2
97.8 ft	hspan_wing
26. ft	z_vtail
100 ft	l_vtail
225.2 ft	length_fuse
8.4 ft	dia_nacelle
27.31 ft	cbar

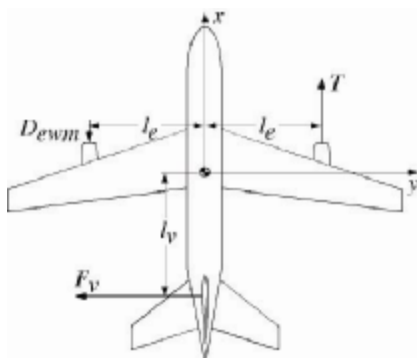


Figure (1) " Engine out geometry"

Figure (2) Boeing 747-400 views with specific important data, [2]

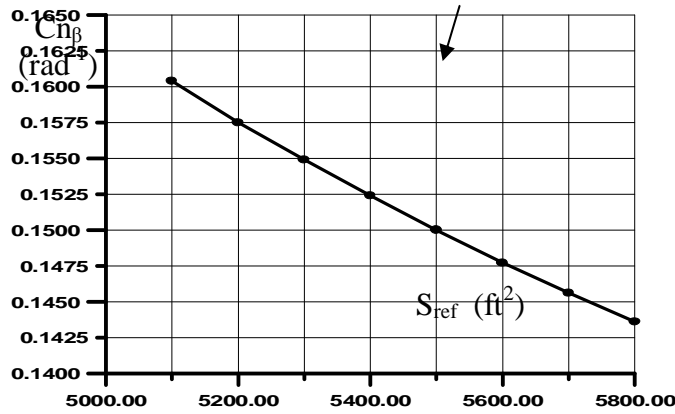


Figure (3) Relation between  $C_{n\beta}$  and Wing Reference Area

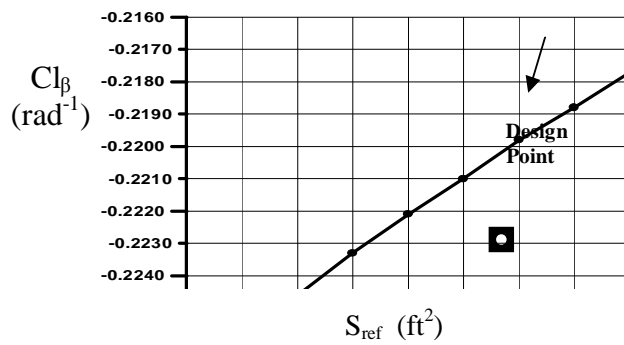


Figure (4) Relation between  $Cl_{\beta}$  and Wing Reference Area

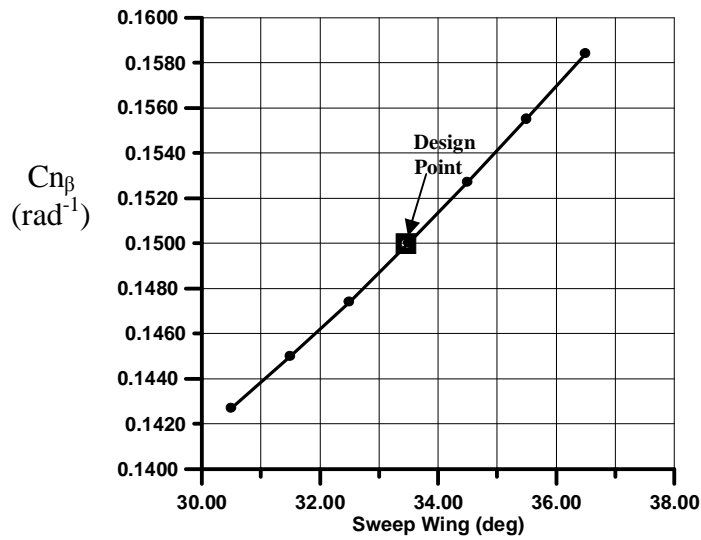


Figure (5) Relation between  $C_{n\beta}$  and Wing Sweep angle

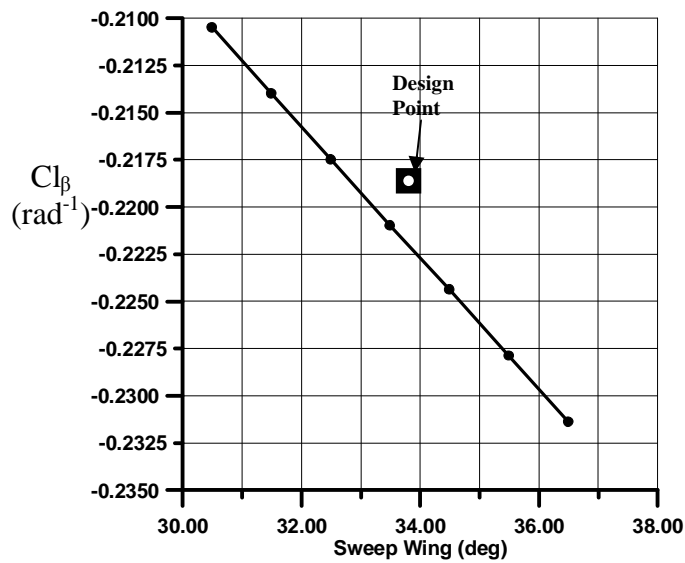


Figure (6) Relation between  $C_{l_\beta}$  and Wing Sweep Angle

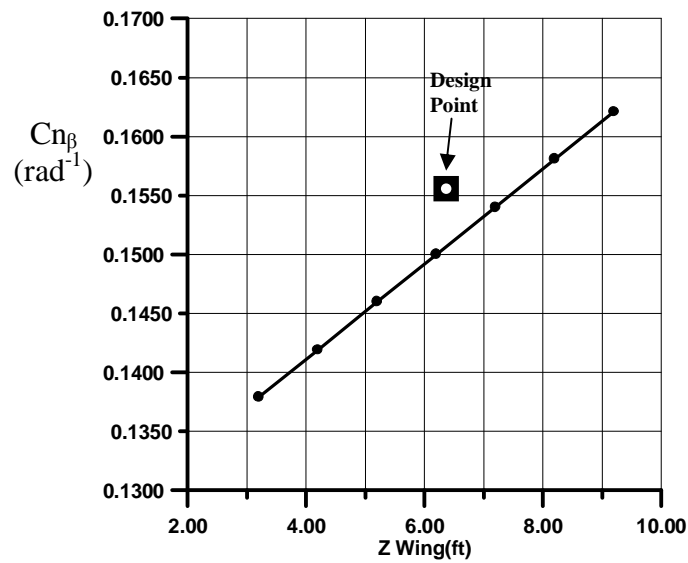


Figure (7) Relation between  $C_{n_\beta}$  and Wing Location

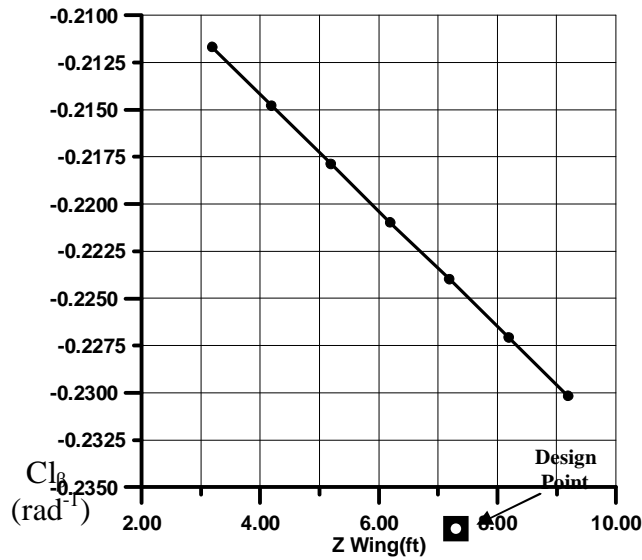


Figure (8) Relation between  $Cl_{\beta}$  and Wing Location

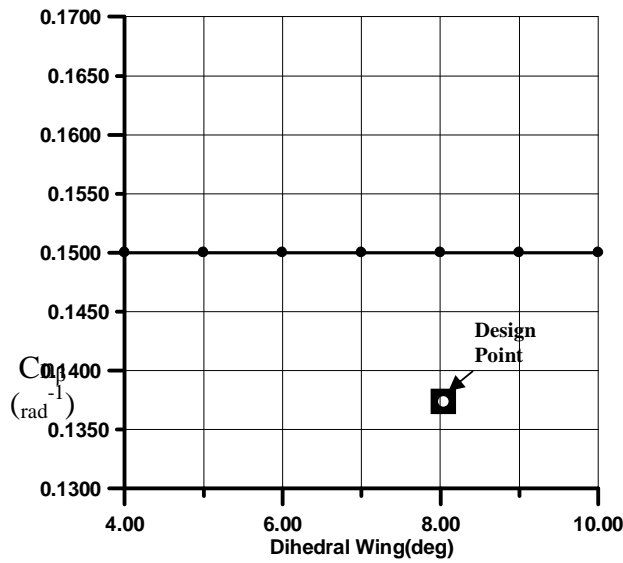


Figure (9) Relation between  $Cn_{\beta}$  and Wing Dihedral

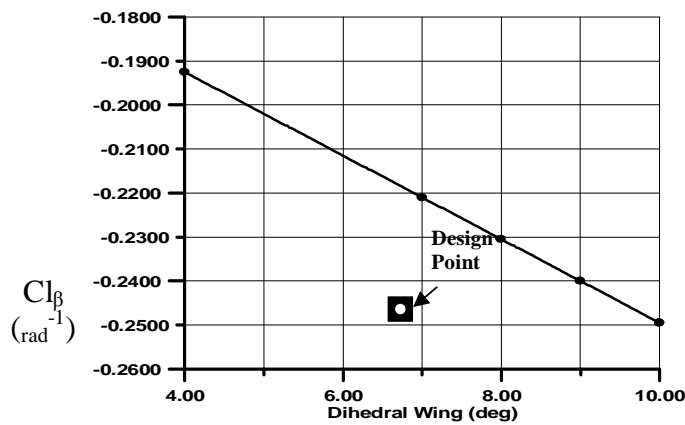


Figure (10) Relation between  $Cl_{\beta}^r$  and Wing Dihedral

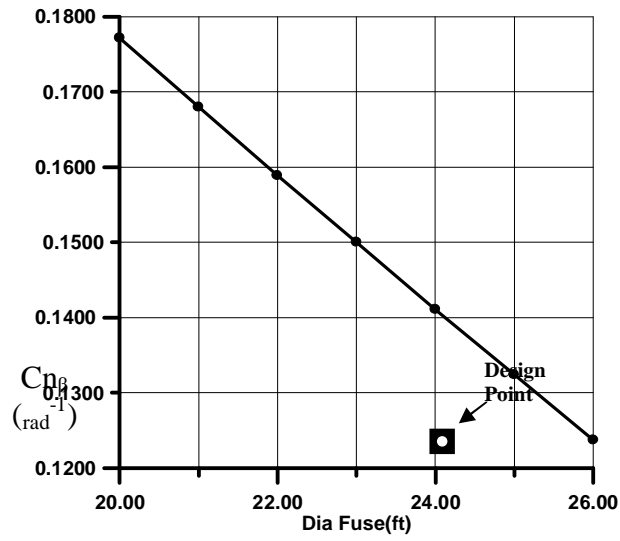


Figure (11) Relation between  $C_{n\beta}$  and Fuselage Diameter

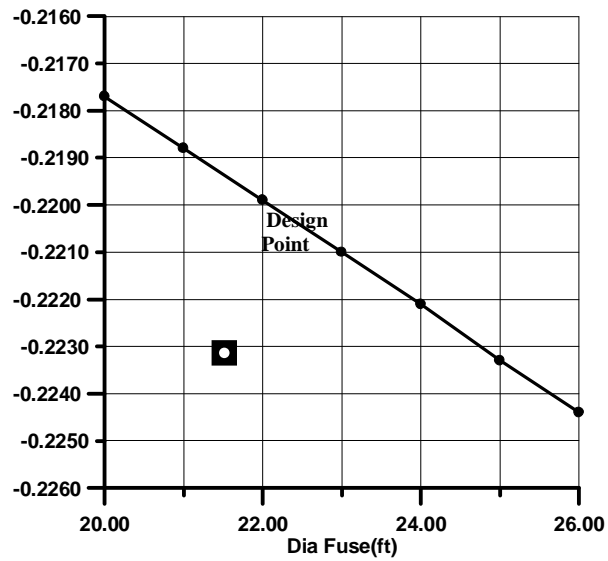


Figure (12) Relation between  $Cl_\beta$  and Fuselage Diameter

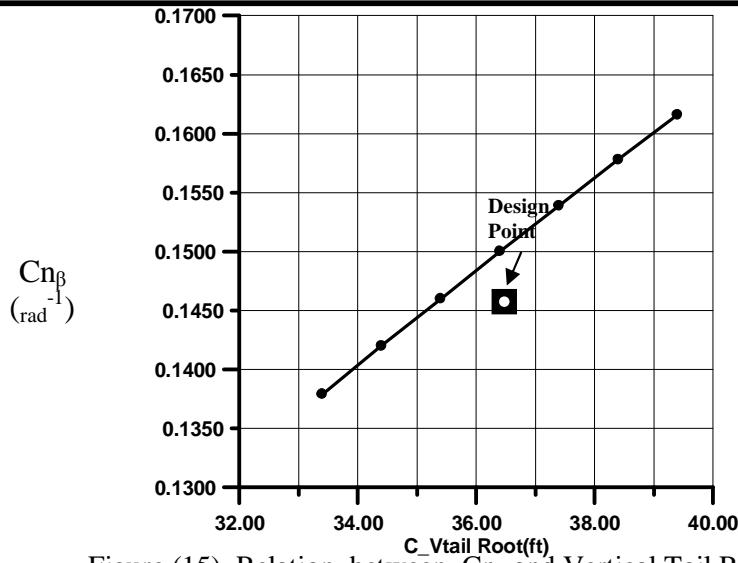


Figure (15) Relation between  $C_{n_\beta}$  and Vertical Tail Root Chord

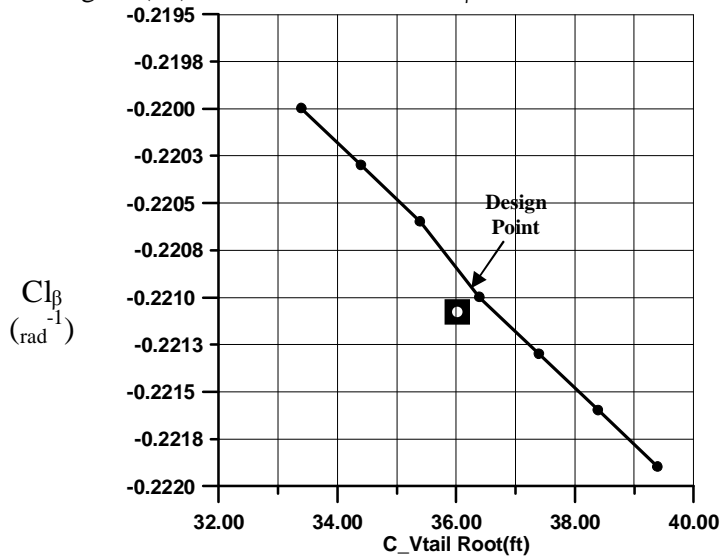


Figure (16) Relation between  $Cl_\beta$  and Vertical Tail Root Chord

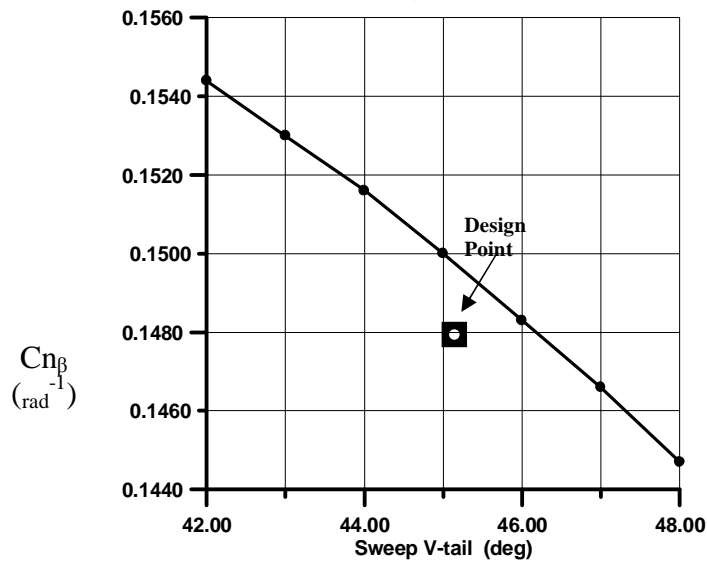
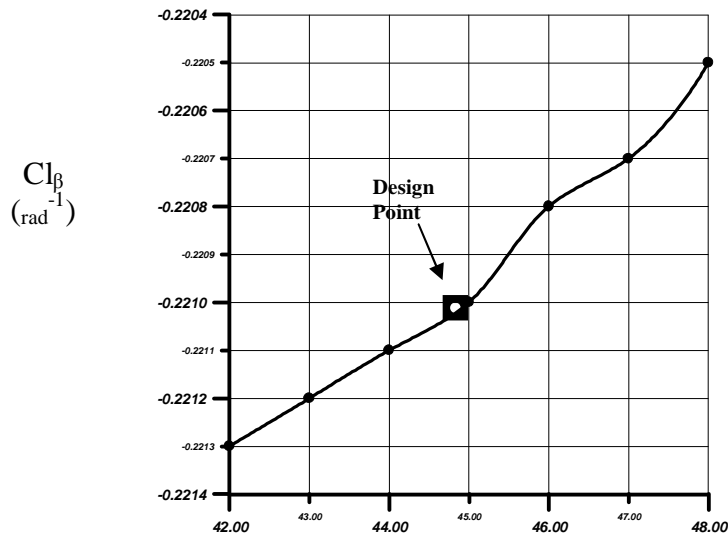


Figure (17) Relation between  $C_{n_\beta}$  and Vertical Tail Sweep Angle



Sweep v-tail (deg)

Figure (18) Relation between  $C_{l_\beta}$  and Vertical Tail Sweep Angle

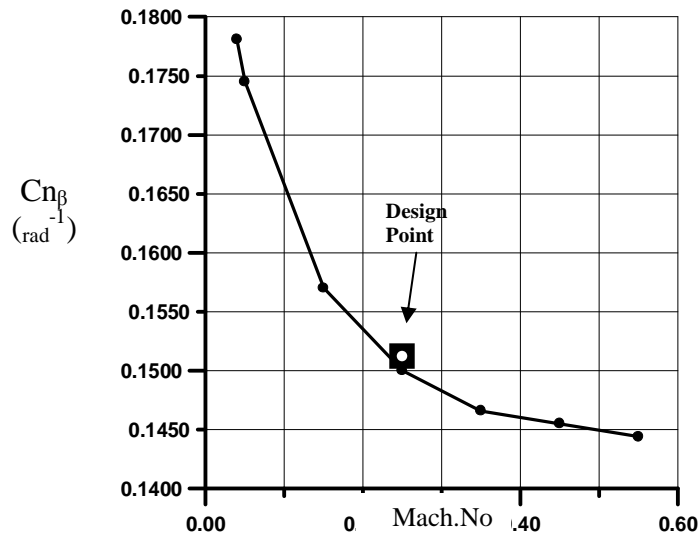


Figure (19) Relation between  $C_{n_\beta}$  and Mach No.

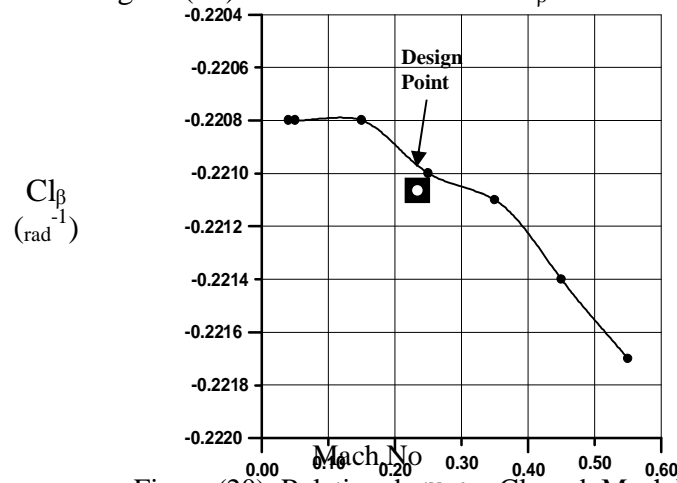


Figure (20) Relation between  $C_{l_\beta}$  and Mach No.